

Adhesion of microcapsules

Peter Graf, Reimar Finken, and Udo Seifert

II. Institut für Theoretische Physik, Universität Stuttgart, 70550 Stuttgart, Germany

The adhesion of microcapsules to an attractive contact potential is studied theoretically. The axisymmetric shape equations are solved numerically. Beyond a universal threshold strength of the potential, the contact radius increases like a square root of the strength. Scaling functions for the corresponding amplitudes are derived as a function of the elastic parameters.

PACS numbers: 68.35.Np, 82.70.Dd, 46.70.Hg

Introduction. – Microcapsules are hollow closed elastic capsules experimentally prepared as layered polyelectrolyte sheets¹ or through polymerization of surfactants coated on oil droplets immersed in aqueous solution². Their elastic constants have been measured by atomic force microscopy^{3,4,5,6}, deformation in shear flow⁷ or osmotically induced swelling^{8,9}. For potential applications not only the knowledge of their elastic constants is crucial, but also, in particular, the understanding of their adhesive properties to other capsules or membranes, to substrates^{10,11} or channel walls¹² in microfluidic devices. In a first systematic experimental study of adhesion to glass surfaces using reflection interference contrast microscopy, adhesion radii were measured as a function of capsule size and membrane thickness¹³. A systematic theory of such deformed shapes, however, is lacking. The analysis of this experiment as well as previous theoretical approaches are adaptations of the standard textbook treatment which involves basically a scaling estimate of the deformation ignoring what are supposed to be factors of order unity¹⁴. Such a simple approach predicts that for small deformations the adhesion radius scales as the square root of the strength of the potential. On the other hand, in the related problem of the adhesion of *fluid* vesicles dominated by curvature elasticity, a systematic solution based on solving numerically variational shape equations has shown that adhesion requires a threshold strength of the potential¹⁵. A priori, there is no reason to believe that this threshold vanishes if a finite shear elasticity is invoked in contrast to the predictions based on the simple scaling picture.

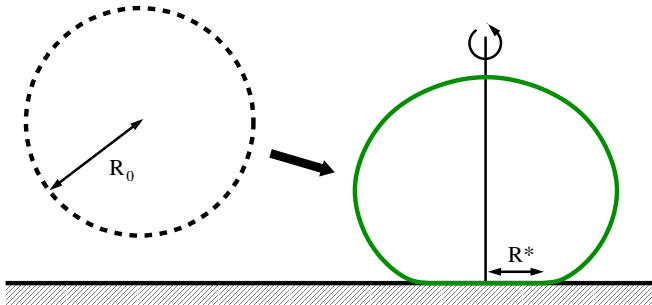


FIG. 1: Spherical microcapsule with radius R_0 undergoes an adhesion transition to an axisymmetric shape with adhesion radius R^* .

In this letter, we investigate systematically the adhesion of microcapsules in a contact potential by solving the corresponding shape equations. We will restrict our treatment to axis-symmetric shapes, see Fig. 1. We therefore exclude configurations where the adhesion area buckles inwards. Such configurations have been observed in recent simulations where, however, the range of the potential was comparable to the size of the capsules^{16,17}. As a main qualitative result, we indeed find that a finite universal threshold strength is required to induce adhesion beyond which the adhesion radius scales like a square root in the excess strength. The amplitude depends strongly on the elastic parameters.

Model. – As an initial reference shape, we choose a sphere of radius R_0 . Any deformation of this sphere costs an elastic energy

$$F_s = \oint dA \left(\frac{\lambda}{2} (u_l^i)^2 + \mu (u_k^i)^2 \right) \quad (1)$$

where λ and μ are the two-dimensional Lamé coefficients, $K = \lambda + \mu$ is the compression modulus, and u_k^i are the elements of the strain tensor^{14,18}. This relation is valid as long as Hooke's law holds. The total energy of the capsule then reads

$$F = F_s + \frac{\kappa}{2} \oint dA (2H - C_0)^2 - W A^*. \quad (2)$$

The second term is the bending energy of the membrane where H is the local mean curvature and κ the bending rigidity. Such a term is required to prevent sharp kinks in an adhesion geometry. We also introduce a spontaneous curvature $C_0 = 2/R_0$ so that the original undeformed spherical capsule has no elastic energy whatsoever. Generally a capsule can be adequately described by these thin shell equations as long as the shell thickness is much smaller than the radius. This assumption is generally fulfilled for capsules larger than a few microns. The third term is the standard adhesion energy in a contact potential of strength W where $A^* \equiv \pi R^{*2}$ is the contact area.

The shape equations for this model can be derived by first parameterizing an axisymmetric shape appropriately and then setting the first variation of F to zero. This procedure can follow closely the corresponding one for fluid vesicles with the additional feature that for an elastic

capsule tangential displacements have a physical significance whereas for fluid vesicles they correspond to irrelevant reparameterizations of the shape and can thus be ignored¹⁹. The technical details will be published elsewhere.

The solutions of these shape equations and hence the “phase diagram” of adhesion depend on three dimensionless parameters

$$k \equiv \frac{KR_0^2}{\kappa}, \quad m \equiv \frac{\mu R_0^2}{\kappa}, \quad w \equiv \frac{WR_0^2}{\kappa} \quad (3)$$

where k and m are the scaled compression and shear modulus, respectively, whereas w is the scaled adhesion energy. In this way, all energies are referred to the scale of the bending energy. While typically $k, m \gg 1$, the scaled adhesion energy can easily be of order 1. Note that we have not implied any volume constraint since at least for the polyelectrolyte shells the membrane is supposed to be water permeable. Introducing such a volume constraint, however, would not pose any fundamental complication but would add one more dimension to the phase diagram.

Adhesion radius. – By solving the shape equations numerically, we find universally that the (scaled) adhesion radius of weakly adhered shapes behaves as

$$r^* \equiv R^*/R_0 \approx a(k, m)(w - w_c)^{1/2}. \quad (4)$$

The critical strength of adhesion $w_c = 2$ is independent of the elastic parameters and indeed the same as found for fluid vesicles without a volume constraint¹⁵. For a weaker contact potential, the potential energetic gain of an adhesion disc is smaller than the cost in curvature energy to be paid. This balance is not modified by the elastic energies.

The dependence of the amplitude $a(k, m)$ on the elastic parameters is best discussed in several steps. For a capsule without shear elasticity, $m = 0$, the amplitude $a(k, 0)$ decreases monotonically with k from the value

$$a_0 \equiv a(0, 0) \simeq 0.58 \quad \text{to} \quad a_\infty \equiv a(k \rightarrow \infty, 0) \simeq 0.50. \quad (5)$$

For $k = 0$, the presence of the non-zero spontaneous curvature energy stabilizes a finite size of the contact radius. For $k \rightarrow \infty$, the model corresponds to that of a fluid vesicle with area constraint. Both limit cases can therefore be checked independently using the shape equations of fluid vesicles without and with area constraint, respectively. Note that without shear elasticity, increasing the compression modulus from zero to infinity thus leads to a decrease in the adhesion radius of only about 15 percent for any given adhesion strength.

A quantitatively more dramatic effect arises for a non-zero shear modulus. In Fig. 2, the amplitude $a(k, m)$ is shown as a function of k for various values of m . For fixed k , the amplitude decreases with increasing m reaching a finite non-zero limit for $m \rightarrow \infty$. Similarly for fixed m the amplitude also decreases with increasing k and reaches a non-zero value in the limit $k \rightarrow \infty$. The limit $k \rightarrow \infty$ can quite well be fitted by the power law

$$a(k \rightarrow \infty, m) \simeq a_\infty(1 + m/m_c)^{-1/4} \quad (6)$$

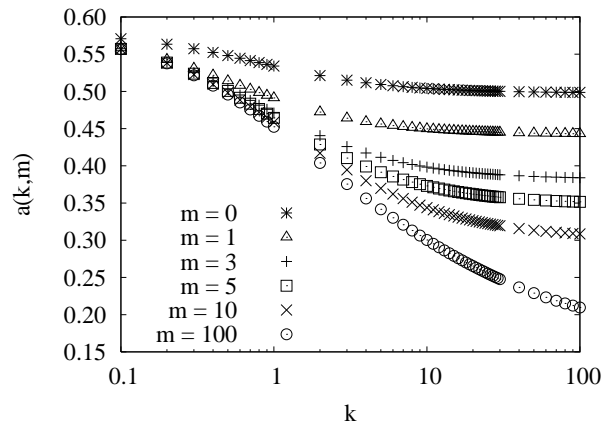


FIG. 2: Amplitude $a(k, m)$ of the adhesion radius (4) as a function of the scaled compression modulus k for various values of the scaled shear modulus m . Note that the abscissa is scaled logarithmically.

with a_∞ given above in eq. (5) and $m_c \simeq 1.54$.

These data for general k and m almost collapse on a scaling plot if these elastic constants are replaced by the (scaled) two-dimensional Young modulus

$$y \equiv \frac{4km}{k+m} \quad (7)$$

and the Poisson ratio

$$\sigma \equiv \frac{k-m}{k+m}. \quad (8)$$

Fig. 3 reveals that the amplitude $a(y, \sigma)$ is almost independent of the Poisson ratio as long as $y \gtrsim 6$, a condition fulfilled if $\min(k, m) \gtrsim 3$. For smaller values of y , the amplitude becomes the larger the smaller σ . Note that all curves have the same limit value $a(y \rightarrow 0, \sigma) \simeq 0.58$ except the curve for $\sigma = 1$. The two cases $k \rightarrow \infty$ and $m = 0$ both correspond to $\sigma = 1$. In the first case the relation $y = 4m$ holds and the amplitude can be calculated directly from eq. (6). In the second case, y is always zero and the amplitude varies from a_0 to a_∞ for increasing k .

For future reference, we extract from our data the fit

$$a(y, \sigma) \simeq \frac{a_\infty}{(1 + y/y_c)^{1/4}} + \frac{a_0 - a_\infty}{(1 + y/\hat{y})^b}. \quad (9)$$

with $\hat{y} = 1.85(1 - \sigma) + 5.58(1 - \sigma)^3$ and $b = 0.98 + 1.42(1 - \sigma) + 2.71(1 - \sigma)^3$. The first term is based on the incompressible case (6) discussed above with the crossover value $y_c \simeq 6.14$. The deviations for small $y \leq 6$ are contained in the second term. This form provides a decent fit with a maximal deviation of 2 percent for all data shown in Fig. 3.

Comparison to experimental data. – Our theory can now be used to reanalyse experimental data. Recently El-sner et al.¹³ investigated the adhesion of polyelectrolyte

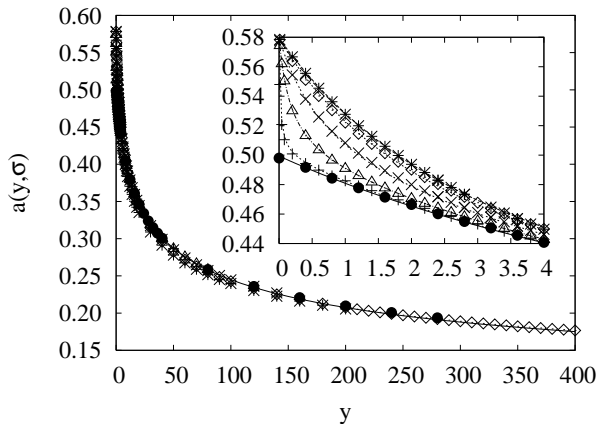


FIG. 3: Amplitude $a(y, \sigma)$ for different values of σ : $\sigma = -1$ (*), $\sigma = 0$ (\diamond), $\sigma = 0.6$ (\times), $\sigma = 0.9$ (\triangle), $\sigma = 0.99$ (+), $\sigma = 1$ (\bullet). For $y \gtrsim 6$ the plots almost collapse on a master curve. For $y \lesssim 6$ a stronger dependence on σ arises. The continuous lines are fits to the data points according to eq. (9).

multilayer capsules (PMCs) on a glass surface. PMCs can be prepared with well-defined shell thickness, shell radius and surface energy. Therefore they are an ideal system to study the adhesive properties of microcapsules experimentally. The contact area and the form of the adhered capsules were reconstructed by reflection interference contrast microscopy. Given the two material properties Young modulus and Poisson ratio the contact potential can be derived by fitting data sets of the contact radius vs. the capsule's wall thickness with fixed capsule's radius or the contact radius vs. the capsule's radius with fixed capsule's wall thickness, respectively.

For thin isotropic shells of thickness h and three-dimensional Young modulus Y_3 the two-dimensional parameters are given by^{14,18}

$$Y = Y_3 h \quad \text{and} \quad \kappa = \frac{Y_3 h^3}{12(1 - \sigma^2)}. \quad (10)$$

Expressing eq. (4) in these variables, we have for large $y \gg y_c$

$$R^* \approx a_\infty (12(1 - \sigma^2)y_c)^{1/4} \left(\frac{R_0^3}{Y_3 h^2} \right)^{1/2} (W - W_c)^{1/2} \quad (11)$$

with

$$W_c \equiv \frac{Y_3 h^3}{6(1 - \sigma^2)R_0^2} \quad (12)$$

for the critical adhesion energy. The large y limit is appropriate since $y = 12(1 - \sigma^2)R_0^2/h^2 \simeq 10^6$ in these experiments.

First, we compare our result to capsules with fixed shell thickness $h = 25.4$ nm and varying capsule's radius R_0 and contact radius R^* . In Fig. 4, the experimental data from Ref. (13) are shown. Using typical experimental values for R^* and R_0 we can estimate $w - w_c$ to be

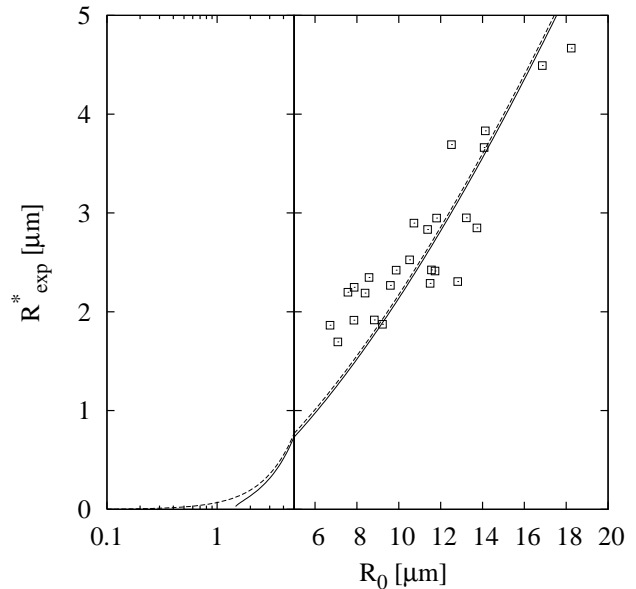


FIG. 4: Comparison of experimental data (\square , from Ref. (13)) to the fit of eq. (11) with $W_c = 0$ (dashed line) and to the fit of eq. (11) for finite $W_c = 9 \mu\text{J}/\text{m}^2$ as extracted from experimental data using the parameters $Y_3 = 294$ MPa, $h = 25.4$ nm, $\sigma = 1/3$, and $R_0 = 10 \mu\text{m}$ (full line). Note that the left part of this figure is scaled logarithmically to better show the influence of the critical adhesion energy W_c .

of the order 100. Thus the critical strength of adhesion can entirely be neglected in eq. (11). Fitting R^* as a function of R_0 with $W_c = 0$ we extract for the combination of adhesion energy, Young modulus and Poisson ratio the estimate $W \simeq Y_3/(1 - \sigma^2)^{1/2} \cdot (1.4 \pm 0.1) \cdot 10^{-12}$ m. Estimates of the adhesion energy become possible using experimental values of the elastic constants. The Young modulus of the shell material is (294 ± 30) MPa^{5,6}. (The value given in Ref. (13) is severely overestimated and therefore not used.) The exact value of the Poisson ratio is unknown but it is usually between 1/3 and 1/2. We then get $0.39 \text{ mJ}/\text{m}^2 \lesssim W \lesssim 0.52 \text{ mJ}/\text{m}^2$, choosing these ranges of parameters. The adhesion energies obtained this way are of the same order as the estimates in Ref. (13). In Fig. 4 the capsule's radius varies between 7 and 18 μm . We can therefore estimate the critical adhesion energy W_c to be in the range from 3 $\mu\text{J}/\text{m}^2$ to 24 $\mu\text{J}/\text{m}^2$. In Fig. 4 both the fit with $W_c = 0$ and the behaviour of R^* vs. R_0 for finite W_c are shown for comparison.

Second, we compare our result with capsules with fixed radius $R_0 = 10 \mu\text{m}$ and fit the contact radius R^* as a function of the shell thickness h (data not shown). From these data we obtain $W \simeq Y_3/(1 - \sigma^2)^{1/2} \cdot (1.3 \pm 0.8) \cdot 10^{-12}$ m, in accordance with the previous estimate.

Summary. – We have solved the shape equation numerically for elastic microcapsules with finite shear elasticity adhering to a contact potential. We have identified a threshold strength required for adhesion. For stronger

potentials the adhesion radius increases like a square root with an amplitude depending on elastic constants which we here determined over the full range of possible parameters.

Acknowledgement. – Financial support of the DFG within the priority program SPP 1164 “Nano- and microfluidics” is gratefully acknowledged.

-
- (1) Donath, E.; Sukhorukov, G. B.; Caruso, F.; Davis, S. A.; Möhwald, H. *Angew. Chem., Int. Ed.* **1998**, *37*, 2202.
 - (2) Rehage, H.; Husmann, M.; Walter, A. *Rheol. Acta* **2002**, *41*, 292–306.
 - (3) Fery, A.; Dubreuil, F.; Möhwald, H. *New J. Phys.* **2004**, *6*, 18.
 - (4) Lulevich, V. V.; Adrienko, D.; Vinogradova, O. I. *J. Chem. Phys.* **2004**, *120*, 3822.
 - (5) Mueller, R.; Köhler, K.; Weinkamer, R.; Sukhorukov, G. B.; Fery, A. *Macromolecules* **2005**, *38*, 9766–9771.
 - (6) Elsner, N.; Dubreuil, F.; Weinkamer, R.; Wasicek, M.; Fischer, F. D.; Fery, A. *Progr. Colloid Polym. Sci.* **2006**, *132*, 117–123.
 - (7) Walter, A.; Rehage, H.; Leonhard, H. *Colloid Polym. Sci.* **2000**, *278*, 169–175.
 - (8) Gao, C.; Donath, E.; Moya, S.; Dudnik, V.; Möhwald, H. *Eur. Phys. J. E* **2001**, *5*, 21–27.
 - (9) Vinogradova, O. I.; Adrienko, D.; Lulevich, V. V.; Nord-schild, S.; Sukhorukov, G. B. *Macromolecules* **2004**, *37*, 1113–1117.
 - (10) Schwarz, U. S.; Komura, S.; Safran, S. A. *Europhys. Lett.* **2000**, *50*, 762–768.
 - (11) Nolte, M.; Fery, A. *Langmuir* **2004**, *20*, 2995.
 - (12) Cordeiro, A. L.; Coelho, M.; Sukhorukov, G. B.; Dubreuil, F.; Möhwald, H. *J. Colloid Interf. Sci.* **2004**, *280*, 68–75.
 - (13) Elsner, N.; Dubreuil, F.; Fery, A. *Phys. Rev. E* **2004**, *69*, 031802.
 - (14) Landau, L. D.; Lifschitz, E. M. *Theory of Elasticity*; Pergamon Press: Oxford, 1970.
 - (15) Seifert, U.; Lipowsky, R. *Phys. Rev. A* **1990**, *42*, 4768.
 - (16) Tamura, K.; Komura, S.; Kato, T. *J. Phys.: Condens. Matter* **2004**, *16*, L421–L428.
 - (17) Komura, S.; Tamura, T.; Kato, T. *Eur. Phys. J. E* **2005**, *18*, 343–358.
 - (18) Boal, D. *Mechanics of the cell*; Cambridge University Press, 2002.
 - (19) Seifert, U. *Adv. Phys.* **1997**, *46*, 13–137.